



**HAL**  
open science

# A Study of the Role of the Parameterization of Heterogeneous Ice Nucleation for the Modeling of Microphysics and Precipitation of a Convective Cloud

T. Hiron, A. Flossmann

► **To cite this version:**

T. Hiron, A. Flossmann. A Study of the Role of the Parameterization of Heterogeneous Ice Nucleation for the Modeling of Microphysics and Precipitation of a Convective Cloud. *Journal of the Atmospheric Sciences*, 2015, 72 (9), pp.3322 - 3339. 10.1175/JAS-D-15-0026.1 . hal-01903788

**HAL Id: hal-01903788**

**<https://uca.hal.science/hal-01903788>**

Submitted on 12 Nov 2021

**HAL** is a multi-disciplinary open access archive for the deposit and dissemination of scientific research documents, whether they are published or not. The documents may come from teaching and research institutions in France or abroad, or from public or private research centers.

L'archive ouverte pluridisciplinaire **HAL**, est destinée au dépôt et à la diffusion de documents scientifiques de niveau recherche, publiés ou non, émanant des établissements d'enseignement et de recherche français ou étrangers, des laboratoires publics ou privés.



Distributed under a Creative Commons Attribution 4.0 International License

# A Study of the Role of the Parameterization of Heterogeneous Ice Nucleation for the Modeling of Microphysics and Precipitation of a Convective Cloud

T. HIRON

*Université Clermont Auvergne, Université Blaise Pascal, Laboratoire de Météorologie Physique, Aubière, France*

A. I. FLOSSMANN

*Université Clermont Auvergne, Université Blaise Pascal, and CNRS, INSU, UMR 6016, Laboratoire de Météorologie Physique, Aubière, France*

(Manuscript received 19 January 2015, in final form 31 March 2015)

## ABSTRACT

Even though ice formation mechanisms in clouds probably obey all the same thermodynamic principles, the associated mechanical and thermal energy transfers differ with respect to the exact pathway and the associated phases. Consequently, heterogeneous ice nucleation parameterizations play an important role in cloud modeling.

The 1.5D bin-resolved microphysics Detailed Scavenging Model (DESCAM) was used to assess the role of the parameterizations for different ice initiation processes. Homogeneous nucleation, deposition freezing, contact freezing, immersion freezing, and condensation freezing were treated explicitly, and their impacts alone and in competition with each other on cloud microphysics and precipitation were studied. The role of efficiently ice-nucleating bacteria on cloud evolution was addressed, as well as means to consider different chemical natures of ice nucleation particles.

For the conditions studied, it was found that deposition and contact freezing only played a negligible role with respect to the other ice-nucleating mechanisms. Homogeneous freezing and classical immersion freezing showed a similar behavior. Both freezing rates increase with increasing drop age (i.e., size). This suggests a possibility for regrouping processes in future parameterized cloud models. Condensation freezing parameterization, however, acts at much warmer temperatures in clouds and for much smaller drops. The associated release of latent heat at lower altitudes caused significantly different cloud dynamics with respect to homogeneous/immersion freezing. This suggests that, in future parameterized models, the condensation freezing process needs particular attention, as well as the fact that ice-forming nuclei (IN) are a subset of aerosol particles that are depleted and replenished like the rest of the population.

## 1. Introduction

Cloud hydrometeors can be either liquid or solid. While knowledge has greatly advanced regarding the formation of liquid drops on a subset of atmospheric aerosol particles called cloud condensation nuclei (CCN) [see, e.g., chapter 9.1 of Pruppacher and Klett (1997)], the understanding regarding the formation of ice particles is still rather patchy. It is commonly admitted that ice crystals are formed via either homogeneous or heterogeneous nucleation.

Homogeneous nucleation refers to the fact that just one phase, here the liquid phase, participates in the ice formation (American Meteorological Society 2015). The designation refers, thus, to a liquid droplet containing potentially dissolved and undissolved species, where, however, only the dissolved species may influence the freezing process. This freezing process organizes the water molecules into an ice lattice and will only be effective at rather low temperatures (generally below  $-36^{\circ}\text{C}$ ), which are commonly found high up in the atmosphere in cirrus cloud regions (e.g., Tabazadeh et al. 2000; DeMott et al. 1997; Koop et al. 2000). Recent studies (e.g., Cziczo et al. 2013; Cziczo and Froyd 2014) have, however, suggested that also in these regions heterogeneous nucleation might dominate.

---

*Corresponding author address:* A. I. Flossmann, Université Clermont Auvergne/INSU, LaMP, 4 Ave. Blaise Pascal, 63178 Aubière, CEDEX, France.  
E-mail: a.flossmann@opgc.univ-bpclermont.fr

Heterogeneous nucleation refers to the process where a second phase (i.e., the solid phase) is necessary for ice formation. This solid phase is provided by a second substance, which is the undissolved part of atmospheric aerosol particles present inside the liquid phase or outside, serving as the organizing surface for the forming ice lattice. These aerosol particles, which form a subset of the overall atmospheric aerosol population, are called ice-forming nuclei (IN). Pruppacher and Klett (1997, chapter 9.2.3) compiled evidence that IN need to have a size larger than  $0.1\text{-}\mu\text{m}$  radius to be effective in initiating ice. They also stressed the role of the insolubility of IN, the role of chemical bond requirements (water must be able to make chemical bonds with the IN surface), and the importance of a crystallographic structure of the IN that templates ice. These requirements favor IN from mineral dusts, biological species (pollen, bacteria, fungal spores, and plankton), carbonaceous combustion products, and volcanic ash (e.g., Szyrmer and Zawadzki 1997; Murray et al. 2012; Baustian et al. 2012). To activate their IN potential, decreasing temperature, ice nucleus diameter and/or surface, and contact angle seem to be dominant factors (e.g., Pruppacher and Klett 1997; Ervens and Feingold 2013), even though some publications seem to suggest that time is also important (Westbrook and Illingworth 2013; Wright and Petters 2013). Review publications have recently summarized the current state-of-the-art knowledge about IN (see, e.g., Hoose and Möhler 2012; Ladino Moreno et al. 2013; Murray et al. 2012).

Even though the thermodynamic principles of germ formation and evolution are probably the same in each heterogeneous nucleation process, the respective mechanical conditions and sensible and latent heat exchanges vary so that, in the literature, different “modes” are distinguished, depending on the exact pathway of interaction between the gaseous, the liquid, and the solid phase during ice formation. This classification of modes has generally been accepted in the past, even though, in recent laboratory and field experiments, the distinction of some of the different nucleation modes is currently under discussion (Vali et al. 2014), and some of the criteria evolve based, for example, on thermodynamic principles. However, in cloud models, the mechanical and heat balance of each individual germ cannot yet be followed; thus, different freezing mode parameterizations are currently the only possible means to simulate heterogeneous nucleation. This is, in particular, true for numerical weather prediction (NWP) models, which generally treat clouds in a highly simplified way, distinguishing for the liquid phase only between bulk cloud drops and bulk precipitating drops, and which need

adapted parameterizations. The current study analyzes the impact of different types of freezing mode parameterizations on the simulated evolution of a cloud with the objective to identify their spatial and temporal windows of importance. In addition, the study wants to provide guidance for the future development of parameterizations for use in NWP models and point out potential areas for improvement or simplification.

Consequently, in the current study, the freezing mode categories are used the way they are presented in general textbooks. Below, these different modes are summarized individually.

*Deposition nucleation* refers to the process where atmospheric water vapor directly deposits on IN particles. These particles may contain some liquid attached to them, as most atmospheric particles are wettable; however, they are not activated into cloud droplets. Thus, in order for deposition nucleation to occur, the atmospheric water vapor needs to be supersaturated with respect to ice but should be subsaturated above the particle surface with respect to liquid water to avoid masking liquid condensation. Hoose and Möhler (2012) compiled currently existing measurements of deposition nucleation on various IN of different chemical composition. They stress the role of the IN type and ice supersaturation but mention also a reduction of deposition nucleation potential if the IN (e.g., mineral dust) is coated, thus covering the active sites. However, the restriction to dry particles (e.g., Hoose et al. 2010) seems unrealistic, as those generally pertain to laboratory measurements and will rarely be found in the atmosphere.

A second process involving unactivated aerosol particles is *contact nucleation*. Here, airborne IN that collide with supercooled preexisting drops will freeze those. However, as generally IN are larger than  $0.1\ \mu\text{m}$  (Pruppacher and Klett 1997), inside cloud they probably have been activated already during drop nucleation [nucleation scavenging activates generally all particles larger than  $0.1\ \mu\text{m}$  (e.g., Flossmann and Wobrock 2010)]; as such, this process can be expected to be important only in the outside-cloud region, mainly below cloud in a supercooled precipitation. For this process to be active the air should generally be subsaturated with respect to water to allow for an existence of a sufficient number of unactivated aerosol particles. Only very few measurements regarding the contact nucleation process exist that do not allow a definite conclusion regarding IN size and temperature [Hoose and Möhler (2012) and references therein]. However, it is admitted that contact freezing occurs at higher temperatures than some of the other nucleation modes (see, e.g., Ladino Moreno et al. 2013).

*Condensation freezing* (also often called condensation followed by freezing) refers to the process where liquid drops freeze because their CCN are also acting as IN. This can be expected to be an important process, as IN are generally large and, even when completely insoluble and not wettable, should nucleate droplets easily via the Kelvin (size) effect alone. This process will form rather small ice crystals in the region where the air is also preferably supersaturated with respect to ice, to assure further deposition growth of the ice crystals. Parameterizations of condensation freezing were proposed, for example, by Fletcher (1962) as a function of supercooling or by Meyers et al. (1992) as a function of ice supersaturation, resulting, for example, from continuous-flow diffusion chamber measurements. Entering these chambers are unactivated aerosol particles, making the experimental distinction between deposition and condensation freezing difficult. Thus, the parameterization of Meyers et al. (1992), for example, regroups deposition and condensation modes. Often, however, in recent literature, condensation nucleation is rather grouped together with immersion freezing (e.g., Hoose and Möhler 2012; Curry and Khvorostyanov 2012). As pointed out also by Cziczo and Froyd (2014), the two freezing processes are distinguished by the temporal separation of droplet formation and ice nucleation, even if they are both initiated by a germ inside a supercooled liquid and are, thus, often difficult to separate experimentally.

Finally, *immersion freezing* refers here to the process where drops freeze while being transported into colder regions. This decrease in temperature would activate some previously taken-up IN surface and launch the freezing process. The taken-up IN can result from nucleation scavenging of a CCN that did not serve as IN at the drop formation temperature or from impaction scavenging of ambient aerosol particles. As inside and outside of the cloud the drops collide and coalesce among each other, the chance to contain an IN surface increases with increasing drop size. One of the first to study the freezing of drops was Bigg (1953), who proposed a freezing probability as a function of drop volume and time for relatively pure water. This approach was extended later to water containing impurities (e.g., Vali 1994), resulting in parameterization formulas resembling in their formalism those for homogeneous nucleation. More recently, newer values have been proposed (e.g., by Diehl and Wurzler 2004) as a function of the IN type. Next to these more experimentally driven parameterizations, formulas derived from classical nucleation theory have also been proposed (e.g., Curry and Khvorostyanov 2012; Hoose et al. 2010) that consider aerosol surface properties. Murray et al. (2011) and Niemand et al. (2012), for example, proposed a freezing

parameterization based on the IN particle surface, while other parameterizations (e.g., Wright and Petters 2013) depend on temperature time evolution or IN nucleus diameter (Ervens and Feingold 2013).

As mentioned above, the criterion to distinguish between condensation and immersion freezing is the temporal separation of droplet formation and ice nucleation. Obviously, this time lapse is open for discussion. However, as the current study aims to improve the representation of ice formation (e.g., in NWP models) the condensation freezing is associated here with the formation of cloud droplets in regions of high supersaturation, while immersion freezing is associated with more mature drops. Constraints in the model will assure a distinct separation of the two processes.

In addition to the freezing mode, all above-mentioned references stress the importance of the chemical composition of the IN. While mineral dust particles as well as carbonaceous combustion products and volcanic ash are active IN below  $-10^{\circ}\text{C}$ , only biological species (pollen, bacteria, fungal spores, and plankton) are known to act at temperatures above  $-10^{\circ}\text{C}$  (e.g., Szyrmer and Zawadzki 1997; Hoose and Möhler 2012; Murray et al. 2012; Attard et al. 2012; Joly et al. 2013; Vätilingom et al. 2012). Because of their large sizes with micrometer-sized diameters, condensation freezing seems to be their main mode of freezing (Schaupp 2014).

Generally, in laboratory and in situ measurements, it is difficult to distinguish between the different ice formation mechanisms if only final ice concentration and compositions are measured. In particular, in the literature, the distinction between immersion and condensation freezing is not rigorously respected, with authors often lumping them together. In addition, the observed number concentrations of ice crystals are biased as a result of eventually occurring ice multiplication processes occurring naturally in clouds or as an artifact during sampling (e.g., Cziczo and Froyd 2014).

Apart from advancing our general understanding of ice-forming mechanisms in clouds, accurate parameterizations of freezing modes are also essential for cloud modeling and prediction, as currently models are not able to follow the mechanical and heat budgets of individual germs. Numerous studies on the pathways of ice formation can be found in the literature using different dynamical frameworks, ranging from parcel models (e.g., Eidhammer et al. 2010) and 1D models (e.g., Morrison et al. 2005) up to 3D LES (e.g., Fridlind et al. 2007) and global-scale models (e.g., Hoose et al. 2010). They follow cloud microphysics using bulk parameterizations (e.g., Phillips et al. 2009; Hoose et al. 2010) or a size-resolved approach (e.g., Fridlind et al. 2007).

However, often models do not distinguish properly between the ice formation modes, because of the

absence of observed data, but also because of their configuration, as most current models treat aerosol particles, if at all, only in a heavily parameterized and, thus, rather simplified way. In particular, also because of the large geographical variability, their chemical composition is generally not specified. Consequently, the IN number in models is generally only linked to temperature or supersaturation but not to their size and depletion in the atmosphere.

Therefore, for example, [DeMott et al. \(2010\)](#) have compiled from 14 years of measurement a global IN distribution as a function of temperature and the number concentration of particles larger than 0.5 μm in diameter irrespective of nucleation mode. Even though such approaches are very practical for generic simulations, model sensitivity studies (e.g., [Meyers et al. 1992](#); [de Boer et al. 2010](#)) have documented an influence of the nucleation mode parameterization on cloud evolution and precipitation formation. However, to our knowledge, no study exists that compares the possible impact of all above-mentioned nucleation parameterizations while also providing a means to take into account their dependence on IN size, chemical composition, and availability.

The current study aims to advance efforts in this direction by using a bin-resolved microphysics code with explicit treatment of the ice phase and the aerosol particle size and chemical composition ([Flossmann and Wobrock 2010](#)). This model has been extended to an explicit treatment of all of the above-mentioned homogeneous and heterogeneous nucleation modes. A detailed assessment of the impact of different nucleation pathways on cloud evolution will help to identify the importance of a specific mode parameterization and will help to point out potential overlap between the parameterizations. In addition, it will help to reply to the question of what bias can be expected if a

generic ice formation mechanism is used instead of a parameterization of the detailed mechanisms for ice formation.

The study uses a simple convective dynamics case in order to assess the different cloud regions affected by each nucleation mode and their respective potential influence on cloud evolution and rain formation. Secondary ice multiplication processes have been disregarded on purpose in our study in order to focus on the primary ice formation due to each process. Consequently, ice is initiated as a result of different nucleation modes and then freezes the formed liquid drops through riming.

The used IN parameterization formulas have been voluntarily chosen as the traditional ones in order to study the impact of each nucleation mode. Also, in our study, the IN composition generally has not yet been specified, except in two cases where the potential of the current approach for future studies was demonstrated by using kaolinite particles for immersion freezing ([Murray et al. 2011](#)) or bacteria for condensation freezing ([Joly et al. 2013](#)).

Below, the modifications to the Detailed Scavenging Model (DESCAM) code as documented in [Flossmann and Wobrock \(2010\)](#) are detailed. Then the dynamical framework and the sensitivity studies are presented. Conclusions and an outlook to future studies conclude the manuscript.

## 2. The DESCAM module

DESCAM ([Flossmann and Wobrock 2010](#)) is a microphysics module where the information regarding the cloud hydrometeor development is treated in a bin-resolved way. Thus, the liquid water is treated by means of the drop size distribution  $f_d(a)$ , where  $a$  is the radius of the drop:

$$\begin{aligned} \frac{\partial f_d(a)}{\partial t} = & \left. \frac{\partial f_d(a)}{\partial t} \right|_{\text{dyn}} + \left. \frac{\partial f_d(a)}{\partial t} \right|_{\text{act/deact}} + \left. \frac{\partial f_d(a)}{\partial t} \right|_{\text{con/eva}} + \left. \frac{\partial f_d(a)}{\partial t} \right|_{\text{AP, coll, d}} + \left. \frac{\partial f_d(a)}{\partial t} \right|_{\text{d, coal}} \\ & + \left. \frac{\partial f_d(a)}{\partial t} \right|_{\text{d, break}} + \left. \frac{\partial f_d(a)}{\partial t} \right|_{\text{nucl, ice}} + \left. \frac{\partial f_d(a)}{\partial t} \right|_{\text{rim}} + \left. \frac{\partial f_d(a)}{\partial t} \right|_{\text{melt}} . \end{aligned} \tag{1}$$

DESCAM follows explicitly the aerosol particle population by means of an aerosol particle size density distribution function  $f_{\text{AP}a}(r)$ , where  $r$  is the moist radius of the aerosol particle. In the context of the present model study, the model has been extended to consider two different types of aerosol particles: type 1 are the atmospheric background particles on which the cloud develops; type 2 are particles that are isolated in order

to keep track of their particular evolution inside the cloud. These can be IN activated in a particular heterogeneous freezing mode or certain IN particles, such as bacteria (ityp = 1 or 2). Consequently, the number of modeled distribution functions has roughly doubled with respect to the version of [Flossmann and Wobrock \(2010\)](#). The 6 functions of [Flossmann and Wobrock \(2010\)](#) pass now at 11, with

$$\begin{aligned} \frac{\partial f_{\text{APa,ityp}}(r)}{\partial t} = & \left. \frac{\partial f_{\text{APa,ityp}}(r)}{\partial t} \right|_{\text{dyn}} + \left. \frac{\partial f_{\text{APa,ityp}}(r)}{\partial t} \right|_{\text{act/deact}} + \left. \frac{\partial f_{\text{APa,ityp}}(r)}{\partial t} \right|_{\text{con/eva}} \\ & + \left. \frac{\partial f_{\text{APa,ityp}}(r)}{\partial t} \right|_{\text{AP,coll,d}} + \left. \frac{\partial f_{\text{APa,ityp}}(r)}{\partial t} \right|_{\text{nucl,ice}} . \end{aligned} \quad (2)$$

To be able to follow the fate of the taken-up particles in the hydrometeors and to calculate correctly the size response of the aerosol particles to humidity changes,

four additional mass density distribution functions calculate the aerosol mass in each size bin for the aerosol particles in the air  $g_{\text{APa,ityp}}(r)$  and the drops  $g_{\text{APd,ityp}}(a)$ :

$$\begin{aligned} \frac{\partial g_{\text{APa,ityp}}(r)}{\partial t} = & \left. \frac{\partial g_{\text{APa,ityp}}(r)}{\partial t} \right|_{\text{dyn}} + \left. \frac{\partial g_{\text{APa,ityp}}(r)}{\partial t} \right|_{\text{act/deact}} + \left. \frac{\partial g_{\text{APa,ityp}}(r)}{\partial t} \right|_{\text{con/eva}} \\ & + \left. \frac{\partial g_{\text{APa,ityp}}(r)}{\partial t} \right|_{\text{AP,coll,d}} + \left. \frac{\partial g_{\text{APa,ityp}}(r)}{\partial t} \right|_{\text{nucl,ice}} , \quad \text{and} \end{aligned} \quad (3)$$

$$\begin{aligned} \frac{\partial g_{\text{APd,ityp}}(a)}{\partial t} = & \left. \frac{\partial g_{\text{APd,ityp}}(a)}{\partial t} \right|_{\text{dyn}} + \left. \frac{\partial g_{\text{APd,ityp}}(a)}{\partial t} \right|_{\text{act/deact}} + \left. \frac{\partial g_{\text{APd,ityp}}(a)}{\partial t} \right|_{\text{con/eva}} \\ & + \left. \frac{\partial g_{\text{APd,ityp}}(a)}{\partial t} \right|_{\text{AP,coll,d}} + \left. \frac{\partial g_{\text{APd,ityp}}(a)}{\partial t} \right|_{d,\text{coal}} + \left. \frac{\partial g_{\text{APd,ityp}}(a)}{\partial t} \right|_{d,\text{break}} \\ & + \left. \frac{\partial g_{\text{APd,ityp}}(a)}{\partial t} \right|_{\text{nucl,ice}} + \left. \frac{\partial g_{\text{APd,ityp}}(a)}{\partial t} \right|_{\text{rim}} + \left. \frac{\partial g_{\text{APd,ityp}}(a)}{\partial t} \right|_{\text{melt}} . \end{aligned} \quad (4)$$

These density distribution functions describe the changes due to the warm cloud microphysics. For the ice phase, three more density distribution functions are

considered,  $f_i(m_i)$  for the number of ice crystals of mass  $m_i$  and  $g_{\text{APi,ityp}}(m_i)$  for the aerosol particle mass of each ityp in the ice crystal mass  $m_i$ :

$$\frac{\partial f_i(m_i)}{\partial t} = \left. \frac{\partial f_i(m_i)}{\partial t} \right|_{\text{dyn}} + \left. \frac{\partial f_i(m_i)}{\partial t} \right|_{\text{nucl,ice}} + \left. \frac{\partial f_i(m_i)}{\partial t} \right|_{\text{dep/sup}} + \left. \frac{\partial f_i(m_i)}{\partial t} \right|_{\text{AP,coll,i}} + \left. \frac{\partial f_i(m_i)}{\partial t} \right|_{\text{rim}} + \left. \frac{\partial f_i(m_i)}{\partial t} \right|_{\text{melt}} , \quad \text{and} \quad (5)$$

$$\begin{aligned} \frac{\partial g_{\text{APi,ityp}}(m_i)}{\partial t} = & \left. \frac{\partial g_{\text{APi,ityp}}(m_i)}{\partial t} \right|_{\text{dyn}} + \left. \frac{\partial g_{\text{APi,ityp}}(m_i)}{\partial t} \right|_{\text{nucl,ice}} + \left. \frac{\partial g_{\text{APi,ityp}}(m_i)}{\partial t} \right|_{\text{dep/sup}} + \left. \frac{\partial g_{\text{APi,ityp}}(m_i)}{\partial t} \right|_{\text{AP,coll,i}} \\ & + \left. \frac{\partial g_{\text{APi,ityp}}(m_i)}{\partial t} \right|_{\text{rim}} + \left. \frac{\partial g_{\text{APi,ityp}}(m_i)}{\partial t} \right|_{\text{melt}} . \end{aligned} \quad (6)$$

As indicated by the subscript, the different terms treat dynamical changes ( $|_{\text{dyn}}$ ); nucleation of drops ( $|_{\text{act,deact}}$ ) and ice crystals ( $|_{\text{nucl,ice}}$ ), and their deactivation back to aerosol particles; evolution involving phase changes because of condensation and evaporation of drops ( $|_{\text{con,eva}}$ ), deposition and sublimation on ice particles ( $|_{\text{dep,sup}}$ ), and melting ( $|_{\text{melt}}$ ), as well as the collision process between the different reservoirs: ( $|_{\text{AP,coll,d}}$ ) for

aerosol/drop collision, ( $|_{\text{AP,coll,i}}$ ) for aerosol/ice particle collision, ( $|_{d,\text{coal}}$ ) for drop/drop collision/coalescence, and ( $|_{\text{rim}}$ ) for drop/ice particle collision; and, last, breakup of drops ( $|_{d,\text{break}}$ ). The mathematical treatment of the different microphysical terms is summarized in [Flossmann and Wobrock \(2010\)](#). The treatment of the two types of aerosol particles is generally completely independent, except when a cloud hydrometeor

completely evaporates. Then the studied particles in the hydrometeors ( $ityp = 2$ ) can, for example, be added to the background particle spectrum ( $ityp = 1$ ) to account for cloud processing.

The formation of ice crystals ( $I_{nucl,ice}$ ) is now subdivided into homogeneous nucleation ( $I_{nucl,hom}$ ), deposition freezing ( $I_{nucl,dep}$ ), contact freezing ( $I_{nucl,cont}$ ), condensation freezing ( $I_{nucl,cond}$ ), and immersion freezing ( $I_{nucl,immersion}$ ):

$$I_{nucl,ice} = I_{nucl,hom} + I_{nucl,dep} + I_{nucl,cont} + I_{nucl,cond} + I_{nucl,immersion}. \quad (7)$$

Homogeneous nucleation is the only rate that does not need IN. The other four terms in Eq. (7) replace the previous treatment of the ice nucleation in DESCAM

(see, e.g., Monier et al. 2006). All ice nucleation parameterizations are detailed below.

*a. Homogeneous nucleation*

Homogeneous nucleation is treated according to Koop et al. (2000) [see Monier et al. (2006) for details]:

$$\log(J_{hom}) = -906.7 + 8502\Delta a_w - 26924\Delta a_w^2 + 29180\Delta a_w^3,$$

where  $J_{hom}$  is the homogeneous nucleation rate ( $\text{cm}^{-3} \text{s}^{-1}$ ), and

$$\Delta a_w(c, T) = a_w(c^{eff}, T) - a_w^i(T),$$

with

$$a_w^i(T) = \exp\left[\left(210368 + 131.438T - \frac{3.3237310^6}{T} - 41729.1 \ln T\right) \frac{10^7}{RT}\right],$$

where  $R$  is the universal gas constant,  $a_w(c^{eff}, T)$  is the water activity of the solution and can be assimilated into the ambient relative humidity over water, and  $a_w^i(T)$  is the water activity of the solution in equilibrium with the ice phase:

$$\left(\frac{df_d}{dt}\right)_{nucl,hom} = -f_d J_{hom} V_d = -\left(\frac{df_i}{dt}\right)_{nucl,hom}.$$

*b. Deposition and condensation freezing nucleation*

Deposition nucleation is defined as the formation of ice directly from the vapor phase at ice supersaturation. This process needs the presence of IN, which are a subset of the aerosol particles present in the air. Condensation freezing nucleation describes a sequence of events where cloud drops form on CCN, which subsequently act as IN, thereby freezing the droplets. As both processes concern either unactivated or freshly activated aerosol particles and need ice supersaturation, they are treated here in a similar manner.

Following Pruppacher and Klett (1997) and DeMott et al. (2010) for a lower size limit, it is assumed that IN radii exceed  $0.1 \mu\text{m}$ . Also, for condensation freezing, an upper size limit of  $16 \mu\text{m}$  for drops was imposed to minimize overlap with immersion freezing. This limit reflects the separation of the cloud drop category in bulk microphysics models. For the number of IN serving as deposition and condensation freezing nuclei, Meyers et al. (1992) proposed

$$N_{IN,Meyers} = \exp(12.96s_{vi} - 0.639).$$

With  $s_{vi}$  being supersaturation over ice,  $N_{IN,Meyers}$  allows us to calculate the total number of IN ( $I^{-1}$ ) at a given moment. This number is compared to the already present total number of ice crystals. If the number of IN proposed by Meyers et al. (1992) exceeds the number of already formed crystals, then this excess gives the total number of new IN  $N_{IN,nucl,new}$ . These, are divided by

$$N_{IN,max} = \sum_{r>0.1\mu\text{m}}^{r_{max}} f_{APa} + \sum_{a_{min}}^{a<16\mu\text{m}} f_d,$$

where  $N_{IN,max}$  is the total number of aerosol particles present in moist particle sizes larger than  $0.1 \mu\text{m}$  and droplets smaller than  $16 \mu\text{m}$ , which could all potentially serve as IN. Then

$$\left(\frac{\partial f_{APa}}{\partial t}\right)_{nucl,dep} = -f_{APa} \frac{N_{IN,nucl,new}}{N_{IN,max}} \frac{1}{\Delta t} \quad \text{if } r > 0.1 \mu\text{m};$$

$$\left(\frac{\partial f_d}{\partial t}\right)_{nucl,cond} = -f_d \frac{N_{IN,nucl,new}}{N_{IN,max}} \frac{1}{\Delta t} \quad \text{if } a < 16 \mu\text{m};$$

and

$$\left(\frac{\partial f_i}{\partial t}\right)_{nucl,Meyers} = \left(\frac{\partial f_d}{\partial t}\right)_{nucl,cond} + \left(\frac{\partial f_{APa}}{\partial t}\right)_{nucl,dep},$$

with time step  $\Delta t$ , which freezes a uniform fraction of all aerosol particles larger than  $0.1 \mu\text{m}$  and drops smaller than  $a_{max} = 16 \mu\text{m}$  and creates ice crystals of corresponding masses. The simulations were rather insensitive to the

variations of  $a_{\max}$ , as this process is proportional to the number of cloud drops that have their maximum number concentration generally well below  $10\ \mu\text{m}$  in supersaturated regions. For one sensitivity test, it was assumed that IN have to be larger than  $0.5\text{-}\mu\text{m}$  radius.

### c. Contact freezing

During the process of impaction scavenging (collision of drops with nonactivated aerosol particles), at temperatures below freezing, some of the collisions can initiate the ice phase and create new ice crystals. The aerosol particles can thus act as contact freezing nuclei. Their number concentration ( $\text{l}^{-1}$ ) is assumed following Meyers et al. (1992) as

$$N_{\text{IN,cont}} = \exp[0.262(273.15 - T_{\text{drop,mean}}) - 2.80],$$

where  $T_{\text{drop,mean}}$  is the mean cloud drop temperature, which is assumed to be identical to the air temperature.

Again, it is assumed that only particles larger than  $0.1\text{-}\mu\text{m}$  radius can serve as contact nuclei. Their total number is calculated by

$$N_{\text{IN,max}} = \sum_{r>0.1\mu\text{m}}^{r_{\max}} f_{\text{AP}a}.$$

The classical impaction scavenging equations of Flossmann (1986) are, thus, replaced, calculating the fraction of freezing that occurs during the collision of aerosol particles and drops (AP,coll,d), where  $K_{\text{AP}d}$  gives the collection kernel for drop/particle collection:

$$\left(\frac{\partial f_{\text{AP}a}}{\partial t}\right)_{\text{AP,coll,d}} = - \int f_{\text{AP}a} f_d K_{\text{AP}d} dm,$$

$$\left(\frac{\partial g_{\text{AP}a}}{\partial t}\right)_{\text{AP,coll,d}} = - \int g_{\text{AP}a} f_d K_{\text{AP}d} dm,$$

$$\left(\frac{\partial f_d}{\partial t}\right)_{\text{AP,coll,d,cont}} = - \frac{\partial}{\partial m} \left[ \left(\frac{dm}{dt}\right)_{\text{AP,coll,d,cont}} f_d \right] - f_d \int f_{\text{AP}a} \frac{N_{\text{IN,cont}}}{N_{\text{IN,max}}} K_{\text{AP}d} dm_{\text{AP}}, \quad \text{and}$$

$$\left(\frac{\partial g_{\text{AP}d}}{\partial t}\right)_{\text{AP,coll,d,cont}} = - \frac{\partial}{\partial m} \left[ \left(\frac{dm}{dt}\right)_{\text{AP,coll,d,cont}} g_{\text{AP}d} \right] + f_d \int g_{\text{AP}a} \left(1 - \frac{N_{\text{IN,cont}}}{N_{\text{IN,max}}}\right) K_{\text{AP}d} dm_{\text{AP}},$$

with

$$\left(\frac{dm}{dt}\right)_{\text{AP,coll,d,cont}} = \int m_{\text{AP}} f_{\text{AP}a} \left(1 - \frac{N_{\text{IN,cont}}}{N_{\text{IN,max}}}\right) K_{\text{AP}d} dm_{\text{AP}};$$

and

$$\left(\frac{\partial f_i}{\partial t}\right)_{\text{nucl,cont}} = - \frac{\partial}{\partial m_i} \left[ \left(\frac{dm_i}{dt}\right)_{\text{AP,coll,d,cont}} f_i \right] + f_d \int f_{\text{AP}a} \frac{N_{\text{IN,cont}}}{N_{\text{IN,max}}} K_{\text{AP}d} dm_{\text{AP}};$$

$$\left(\frac{\partial g_{\text{AP}i}}{\partial t}\right)_{\text{nucl,cont}} = - \frac{\partial}{\partial m_i} \left[ \left(\frac{dm_i}{dt}\right)_{\text{AP,coll,d,cont}} g_{\text{AP}i} \right] + f_d \int g_{\text{AP}a} \frac{N_{\text{IN,cont}}}{N_{\text{IN,max}}} K_{\text{AP}d} dm_{\text{AP}},$$

with

$$\left(\frac{dm_i}{dt}\right)_{\text{AP,coll,d,cont}} = \int m_{\text{AP}} f_{\text{AP}a} \frac{N_{\text{IN,cont}}}{N_{\text{IN,max}}} K_{\text{AP}d} dm_{\text{AP}}.$$

To study the impact of the lower size limit of IN on the results, for one sensitivity test it was assumed that IN have to be larger than  $0.5 \mu\text{m}$ .

*d. Immersion freezing*

Water drops present in the atmosphere will freeze if the temperature decreases below a critical value. Bigg (1953) pointed out that the larger the drops, the greater the probability that water molecules stick together to form critical ice embryos, which initiate the ice phase. This statistical approach suggests a dependence of the drop freezing process on the drop volume  $V_d$ .

In addition, aerosol particles previously scavenged into the drops contribute salt mass for a freezing temperature depression and insoluble material, which might serve as a freezing nucleus (Diehl and Wurzler 2004). This also suggests a dependence on drop volume, as the mass of scavenged material increases with drop size.

The general formula describing these effects is as follows [see Pruppacher and Klett (1997) for details]:

$$-\frac{1}{N_u} \left( \frac{dN_u}{dt} \right) = \frac{1}{N_u} \left( \frac{dN_f}{dt} \right) = BV_d [\exp(aT_s) - 1],$$

where  $N_u$  and  $N_f$  are the number of unfrozen and frozen drops, respectively, and  $T_s = 273.15 - T_{\text{drop\_mean}}$ . Here,  $T_{\text{drop\_mean}}$  is again replaced by the air temperature until future model development.

For temperatures below  $-5^\circ\text{C}$ , generally the  $-1$  in the parentheses can be neglected and the number of frozen drops in the model can be calculated by

$$\begin{aligned} \left( \frac{df_d}{dt} \right)_{\text{nucl,immersion,vol}} &= -f_d V_d B \exp(aT_s) \\ &= - \left( \frac{df_i}{dt} \right)_{\text{nucl,immersion,vol}}, \quad \text{and} \end{aligned}$$

$$\begin{aligned} \left( \frac{dg_{\text{APd}}}{dt} \right)_{\text{nucl,immersion,vol}} &= -g_{\text{APd}} V_d B \exp(aT_s) \\ &= - \left( \frac{dg_{\text{APi}}}{dt} \right)_{\text{nucl,immersion,vol}}, \end{aligned}$$

which also gives the number of formed ice particles and their aerosol particle mass. Different proposed values of  $a$  and  $B$  can be found in the literature, ranging from the lower limit for purified water proposed by Bigg (1953) ( $a = 0.82 \text{ K}^{-1}$  and  $B = 2.9 \times 10^{-8} \text{ cm}^{-3} \text{ s}^{-1}$ ) to much higher values (e.g., Orville and Kopp 1977). The original values of Bigg (1953) initiate drop freezing at temperatures up to  $-15^\circ\text{C}$ , probably as a result of both dissolved and undissolved aerosol material in the liquid phase. A sensitivity test using the low original Bigg values of  $B$

was made, while generally the 100-times-larger value of  $B = 2.9 \times 10^{-6} \text{ cm}^{-3} \text{ s}^{-1}$  was used, which corresponds to the orders of magnitude of recent observations (e.g., Diehl and Wurzler 2004).

Curry and Khvorostyanov (2012) and Hoose et al. (2010), among others, have pointed out that, instead of using a volume approach, it would be preferable to consider the surface area of the IN inside the drop when estimating the nucleation rate. Murray et al. (2011) thus proposed a parameterization in assuming that the IN is a kaolinite particle. Then the nucleation is calculated from

$$\begin{aligned} \left( \frac{df_d}{dt} \right)_{\text{nucl,immersion,surf}} &= -f_d J_{\text{surf}} \sigma \\ &= - \left( \frac{df_i}{dt} \right)_{\text{nucl,immersion,surf}}, \end{aligned}$$

with  $\sigma$  as the IN surface area and

$$J_{\text{surf}}(T) = \exp(-0.8802T + 222.17)$$

( $\text{cm}^{-2} \text{ s}^{-1}$ ) in the temperature range between 236.1 and 245.5 K.

While the drop volume is readily available in our model, because of the bin-resolved approach, the information of the surface area of IN inside the drop needs additional assumptions, as only the total aerosol particle mass is followed in each drop bin. It will generally be assumed that the kaolinite particle mass present in each drop resulted from 10 CCN particles because of collision and coalescence of drops. A sensitivity test using only 1 CCN particle/drop was also made. Also, it was taken into account that the soluble aerosol particle material does not contribute to the IN surface. Because of their size dependency, both immersion freezing rates are quite small for cloud droplets.

**3. The dynamic framework and its initialization**

For the current study, the DESCAM module was coupled to a 1.5D dynamic framework. The dynamical part of the model is based on the work of Asai and Kasahara (1967), where two concentric cylinders represent the convective cloud and its environment. As the radius of the outer cylinder (36 km) is 10 times the inner one (3.6 km), it was assumed that the strong air motion inside the cloud has a small impact on the environment. Consequently, the environmental variables remain unchanged during the simulation. Only the vertical velocity in the outer cylinder changes with time and describes the compensating downdraft. The inner cylinder, however, follows the vertical variation of temperature, humidity, wind, and cloud elements as

TABLE 1. List of case studies and the results for the cumulative rain on the ground.

Case	Name	Description	Cumulative rain (mm)
Case 1	Reference	All ice nucleation modes active (using the surface immersion freezing parameterization with 10 particles per drop)	11.98
Case 2	All liquid	No ice formation	7.82
Case 3	Deposition	Only deposition freezing active	9.00
		IN > 0.5 μm	7.98
Case 4	Contact	Only contact freezing active	7.80
		IN > 0.5 μm	8.06
Case 5	Immersion	Only immersion freezing active	
		a) with surface parameterization (10 kaolinite particles per drop)	6.22
		b) with surface parameterization (1 kaolinite particle per drop)	6.57
		c) with volume parameterization ( $B = 2.9 \times 10^{-6} \text{ cm}^{-3} \text{ s}^{-1}$ )	4.69
		d) with volume parameterization ( $B = 2.9 \times 10^{-8} \text{ cm}^{-3} \text{ s}^{-1}$ )	7.49
Case 6	Homogeneous	Only homogeneous nucleation active	4.36
Case 7	Condensation	Only condensation freezing active	15.05
Case 8	Bacteria	Only a fraction $\tau$ of bacteria are IN ( <i>Pseudomonas syringae</i> 32b-74) (ityp = 2)	26.75 ( $\tau = 10^{-2}$ )
			11.83 ( $\tau = 10^{-3}$ )

detailed in Leroy et al. (2006). Lateral exchange terms allow, for example, for detrainment of hydrometeors and entrainment of fresh aerosol particles from the environment.

For the simulation, the observation during the Cooperative Convective Precipitation Experiment (CCOPE; Dye et al. 1986), which followed the evolution of a small thunderstorm that occurred in southeastern Montana in 1981, is used. To simulate the 19 July 1981 cumulonimbus, the model is initialized with the vertical sounding of Miles City at 1440 mountain daylight time (MDT), which provides temperature and humidity profiles (Dye et al. 1986); to force convection, a surface heating of 2.3°C is applied during the first 10 min (Leroy et al. 2006).

The aerosol particle distributions are initialized using a superposition of three lognormal number distributions:

$$f_{\text{APa,ityp}=1}(r) = \sum_i \frac{n_i}{\sqrt{2\pi} \ln(10) \log \sigma_i} \exp\left\{-\frac{[\log(r/R_i)]^2}{2(\log \sigma_i)^2}\right\},$$

where  $R_i$  is the mean particle radius,  $n_i$  is the integral of the  $i$ th normal function, and  $\log \sigma_i$  is a measure of spectra width, as proposed by Jaenicke (1988) (see also Hobbs 1993). For the parameters, the values for a continental air mass are used:  $n_i = 997, 842, \text{ and } 0.00071$ ;  $R_i = 0.001, 0.0218, \text{ and } 6.24$ ;  $\log(\sigma_i) = 0.328, 0.505, \text{ and } 0.277$ . For all cases, the background aerosol particle spectrum (ityp = 1) is assumed to be constant in the first kilometer and to decrease above. Generally, it is assumed that the aerosol particles are composed of 90% of  $(\text{NH}_4)_2 \text{SO}_4$  and 10% of an insoluble nucleus (e.g., kaolinite), which serves as IN according to the nucleation parameterizations detailed above.

In the first simulation, all ice-forming processes are active. This will provide the reference case against which the other simulations will be compared (case 1; Table 1). In a second simulation, all ice-forming processes are inactive; thus, all ice formation is suppressed, and only liquid hydrometeors are formed. This simulation yields a second reference for the role of the ice phase (case 2; Table 1).

Different simulations are then performed where only one ice-forming mechanism is kept active. Table 1 summarizes the different sensitivity tests that were performed. Cases 3 to 7 pertain to simulations where each of the possible different nucleation modes is active alone.

Case 8 aims to study the potential impact of the presence of a category of extremely active IN on cloud and rain development. Here, bacteria were selected, as they are known to be the only natural IN that are active also at temperatures warmer than  $-10^\circ\text{C}$  (Szyrmer and Zawadzki 1997).

Burrows et al. (2009) compiled bacterial number concentrations of up to  $1 \text{ cm}^{-3}$  with typical values around  $0.01 \text{ cm}^{-3}$ . Bacteria typically have sizes around  $1 \mu\text{m}$  in diameter and, through their size and wettability, will be CCN before acting as IN. Joly et al. (2013) identified an extremely ice-active strain of bacteria during the biological aerosol particles in the atmosphere and their impact on clouds (BIOCLOUDS) experiments on the Puy de Dôme in France (*Pseudomonas syringae* 32b-74). To obtain an upper limit for the importance of bacteria in cloud ice formation, the observed freezing values were adapted, and ice is assumed to form with a nucleation percentage of 0.05% for  $-2^\circ$  to  $-2.5^\circ\text{C}$ , 2.3% for  $-2.5^\circ$  to  $-3.5^\circ\text{C}$ , 3.7% for  $-3.5^\circ$

to  $-4.5^{\circ}\text{C}$ , and 4.1% for  $-4.5^{\circ}$  and  $-10^{\circ}\text{C}$  [adapted from Fig. 1 of Joly et al. (2013)]. The total number concentrations of bacteria were taken from Burrows et al. (2009), assuming that a fraction  $\tau$  of all bacteria followed the nucleation rates of these *Pseudomonas syringae* 32b-74. The overall bacteria lognormal size distribution (ityp = 2) is

$$f_{APa,bact}(r) = \frac{n}{\sqrt{2\pi} \ln(10) \log\sigma} \exp\left\{-\frac{[\log(r/R)]^2}{2(\log\sigma)^2}\right\},$$

with  $n = 0.35 \text{ cm}^{-3}$ ,  $R = 0.62 \mu\text{m}$ , and  $\sigma = 0.13$  [adapted from Schaupp (2014) and Andraud (2011)].

**4. Results**

The results of DESCAM have already been compared to the CCOPE measurements in the 1.5D framework by Leroy et al. (2006) and yielded a significant amount of rain formation and rainfall rates locally exceeding  $75 \text{ mm h}^{-1}$  (cf. Figs. 1a and 1c). The results of the dynamics and microphysical parameters can be found in Leroy et al. (2006), and most of them will not be repeated here. In the framework of the current study, only the variation of the results because of changes in the ice initiation shall be studied.

Figure 1a displays the time and height evolution of the liquid water content in red and the ice water content in blue. The initial  $0^{\circ}$ ,  $-15^{\circ}$ , and  $-35^{\circ}\text{C}$  levels are indicated to facilitate interpretation. Liquid water starts to form after 8 min around 3-km altitude. Cloud top and liquid water content increase rapidly with time. Some primary ice forms early on above 8-km altitude but only in low quantities. Important contents of ice only appear after the liquid cloud extends above 7-km altitude. Within 25 min, the entire cloud is glaciated. The ice particles fall toward the ground and melt instantaneously at the  $0^{\circ}\text{C}$  level around 3 km. Liquid precipitation reaches the ground around 35 min after cloud formation. The cumulative rainfall amounts to 11.98 mm (Table 1), falling mainly during a 30-min interval (cf. Fig. 1c).

Figure 1b displays the time and height evolution of the liquid water content for the all-liquid case 2, where all formation of ice is suppressed. The early evolution of the cloud stays the same. However, the formation of precipitation-sized hydrometeors is much faster, and the main rain is already falling around 45 min (Fig. 1c) with a peak intensity exceeding  $100 \text{ mm h}^{-1}$ . The main rain stops sooner than in the reference case, and the cumulative precipitation stays below the mixed phase case with 7.82 mm (Table 1). The fact that the ice formation delays precipitation formation has been reported already in the literature (see, e.g., Respondek et al. 1995)

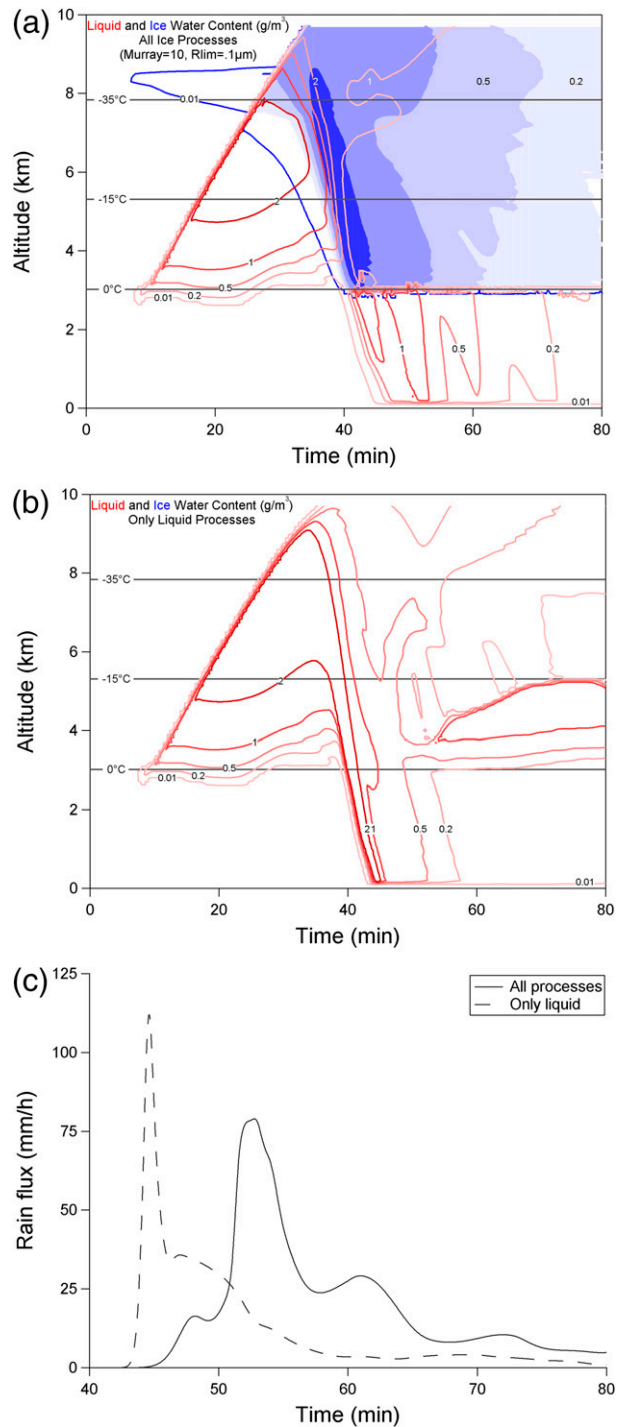


FIG. 1. (a) Liquid water content ( $\text{g m}^{-3}$ ; red) and ice water content ( $\text{g m}^{-3}$ ; blue), simulated with DESCAM as a function of time and height for the reference case 1. (b) Liquid water content ( $\text{g m}^{-3}$ ; red) simulated with DESCAM as a function of time and height for the all-liquid case 2. (c) Time evolution of the rainfall rate ( $\text{mm h}^{-1}$ ) for the reference case 1 (solid) and the all-liquid case 2 (dashed).

and can be attributed to the fact that the release of latent heat of freezing creates additional updraft suspending larger particles and, in addition, ice particles have a lower terminal velocity than liquid hydrometeors because of a reduced density.

Figure 2 displays the results of the sensitivity cases 3 and 4, where only deposition freezing (case 3; Fig. 2a) or only contact freezing (case 4; Fig. 2b) is considered. Both occur because of unactivated aerosol particles in cold regions. From Fig. 2a, it becomes evident that the early ice formation around 8-km altitude observed in the reference case (cf. Fig. 1a) is, in fact, because of the deposition of water vapor on upper-tropospheric aerosol particles. The formed ice particles grow once they collide with drops and form large ice particles that fall and melt on the way to the ground. However, the number of pristine ice particles formed around 8 km is relatively small so that precipitation onset is similar to the all-liquid case 2 (Fig. 2c). Even though the first maximum of rainfall intensity is lower, the integrated value slightly exceeds the one for the all-liquid case 2. Increasing the minimum size of deposition freezing IN from 0.1 to  $0.5 \mu\text{m}$  almost completely eliminates the effect of the ice phase, and the cumulative rain yields a value of 7.98 mm, which is very close to the all-liquid case 2 (results not shown). A similar argumentation applies to the contact freezing case (Fig. 2b), where even less ice is formed. Here, the results for case 4 are almost completely identical to the all-liquid case (Fig. 2c). Increasing the lower IN size to  $0.5 \mu\text{m}$  (Fig. 2b) increases the rain only very little [8.06 vs 7.8 mm for IN limit  $0.1 \mu\text{m}$  (not shown)]. This overall relatively small effect of deposition and contact freezing in the vigorous convective case considered is certainly caused by the specific dynamics and might increase in more stratiform dynamics with longer supercooled outside-cloud periods. In the following, the lower IN size limit was kept as  $0.1 \mu\text{m}$ .

Figure 3 displays the results of the sensitivity cases where two different parameterizations for immersion freezing (case 5) are considered. In Fig. 3a, the surface parameterization rate of immersion freezing was used with 10 same-sized particles making up the total insoluble mass. Figure 3b shows the evolution using the volume immersion freezing parameterization with  $B = 2.9 \times 10^{-6} \text{cm}^{-3} \text{s}^{-1}$ . Two sensitivity tests were done, one with the original Bigg values pertaining to purified water, and one where the surface for freezing was calculated assuming it belongs to only one particle. Both surface and volume-based rates are a function of temperature, occur mainly in the upper parts of the cloud mostly at temperatures below  $-35^\circ\text{C}$ , and increase with increasing drop size (more liquid volume and more

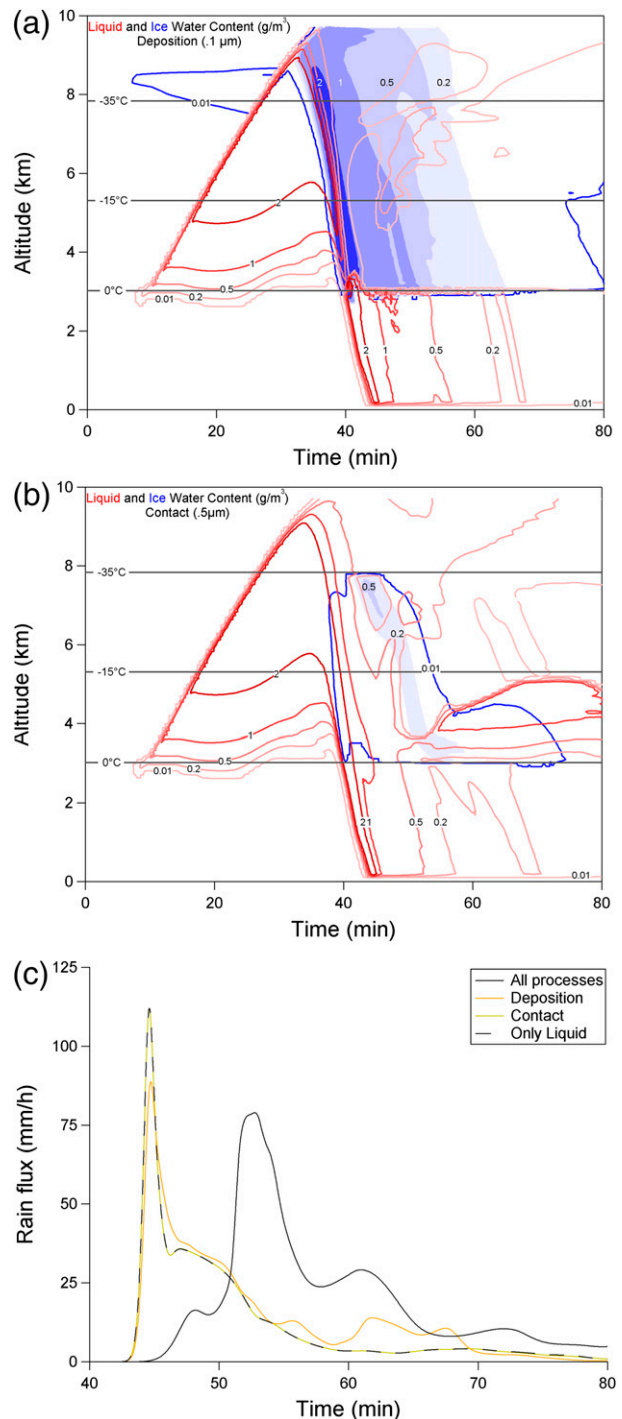


FIG. 2. (a) Liquid water content ( $\text{g m}^{-3}$ ; red) and ice water content ( $\text{g m}^{-3}$ ; blue), simulated with DESCAM as a function of time and height for deposition freezing as the only active ice-forming mechanism (case 3). (b) Liquid water content ( $\text{g m}^{-3}$ ; red) and ice water content ( $\text{g m}^{-3}$ ; blue), simulated with DESCAM as a function of time and height for contact freezing (IN  $> 0.5 \mu\text{m}$ ) as the only active ice-forming mechanism (case 4). (c) Time evolution of the rainfall rate ( $\text{mm h}^{-1}$ ) for the reference case (solid black), the all-liquid case (dashed black), the deposition freezing case 3 (orange), and the contact freezing case 4 (yellow).

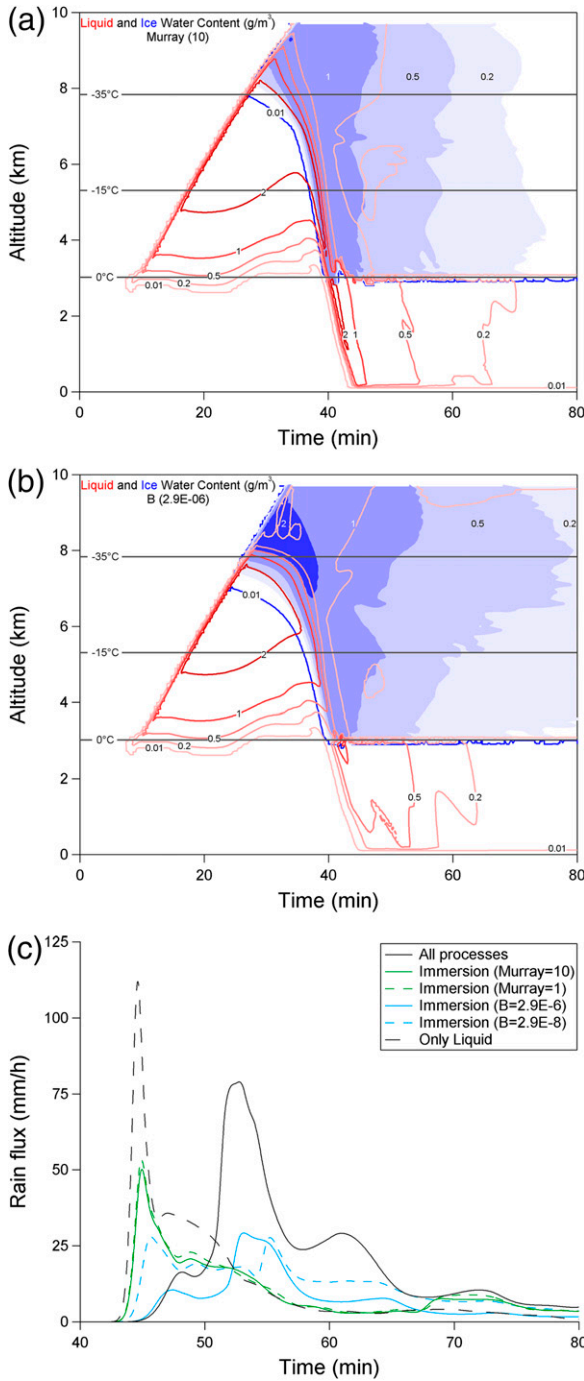


FIG. 3. (a) Liquid water content ( $\text{g m}^{-3}$ ; red) and ice water content ( $\text{g m}^{-3}$ ; blue), simulated with DESCAM as a function of time and height for surface immersion freezing as the only active ice-forming mechanism (case 5a). (b) Liquid water content ( $\text{g m}^{-3}$ ; red) and ice water content ( $\text{g m}^{-3}$ ; blue), simulated with DESCAM as a function of time and height for volume immersion freezing as the only active ice-forming mechanism (case 5c). (c) Time evolution of the rainfall rate ( $\text{mm h}^{-1}$ ) for the reference case (solid black), the all-liquid case (dashed black), the immersion surface freezing rates with 10 particles per drop (solid green) and with 1 particle per drop (dashed green), and the immersion volume freezing rate with  $B = 2.9 \times 10^{-6} \text{ cm}^{-3} \text{ s}^{-1}$  (solid blue) and  $B = 2.9 \times 10^{-8} \text{ cm}^{-3} \text{ s}^{-1}$  (dashed blue).

captured particle mass). They all form ice above 8-km altitude and collide with drops while falling. Concerning the rain flux (Fig. 3c), cases 5a and 5b follow most closely the all-liquid case 2, irrespective of the assumption on the number of IN forming the particle mass, while case 5c with the elevated  $B$  value shows almost no peak in the warm rain formation peak. The immersion freezing case with the low  $B$  value resulting from Bigg (1953) for purified water is situated between the three other curves. The total amount of precipitation is reduced with 6.22 mm for the surface immersion nucleation rate (6.57 for only 1 particle) and 4.69 mm for the volume immersion freezing case (7.49 mm for the low  $B$  value case). From Fig. 3a, for the surface immersion freezing, it can be seen that much less ice was formed above 7 km, and a lot more liquid water stays present, as compared to Fig. 3b. Concerning the sensitivity test of case 5d for low  $B$  values, the ice initiation resembles case 5c with less ice above 7 km. Overall, one notes that the surface and volume immersion freezing have as a common features that they induced freezing mainly for larger drops at high altitudes. Furthermore, most of them did not reproduce the maximum rainfall rate around 55 min for the reference case (Fig. 3c; solid black line), even though the immersion freezing was active for all drops and not just for the larger ones. Only the case with the large  $B$  value showed a maximum precipitation rate around 55 min; however, it was much smaller than for the reference case.

Figure 4 displays the results of the sensitivity cases where only homogeneous freezing (Fig. 4a) and only condensation freezing (Fig. 4b) are considered. The behavior of homogeneous freezing alone extrapolates the behavior of the low parameter volume immersion freezing rate (case 5d), as the ice appears still later and higher up in the cloud. And the rain flux resembles more the all-liquid case with an early maximum around 45 min. The condensation freezing rate, however, displays the largest impact on in-cloud microphysics and rainfall. Figure 4b shows that important ice formation now occurs at all altitudes inside the cloud, including regions where the warm rain process is acting. Here, the riming process now takes over, replacing collision and coalescence of liquid drops, suppressing completely the warm rain peak in Fig. 4c, releasing important quantities of latent heat and causing a much larger rainfall tail with a total of 15.05 mm of rain, exceeding the reference case by around 30%.

Comparing the different parameterization rates, it seems that surface and volume immersion freezing and homogeneous freezing behave somewhat similarly. Even though their physical basis is quite different, they all form ice late and high up in the cloud from aged

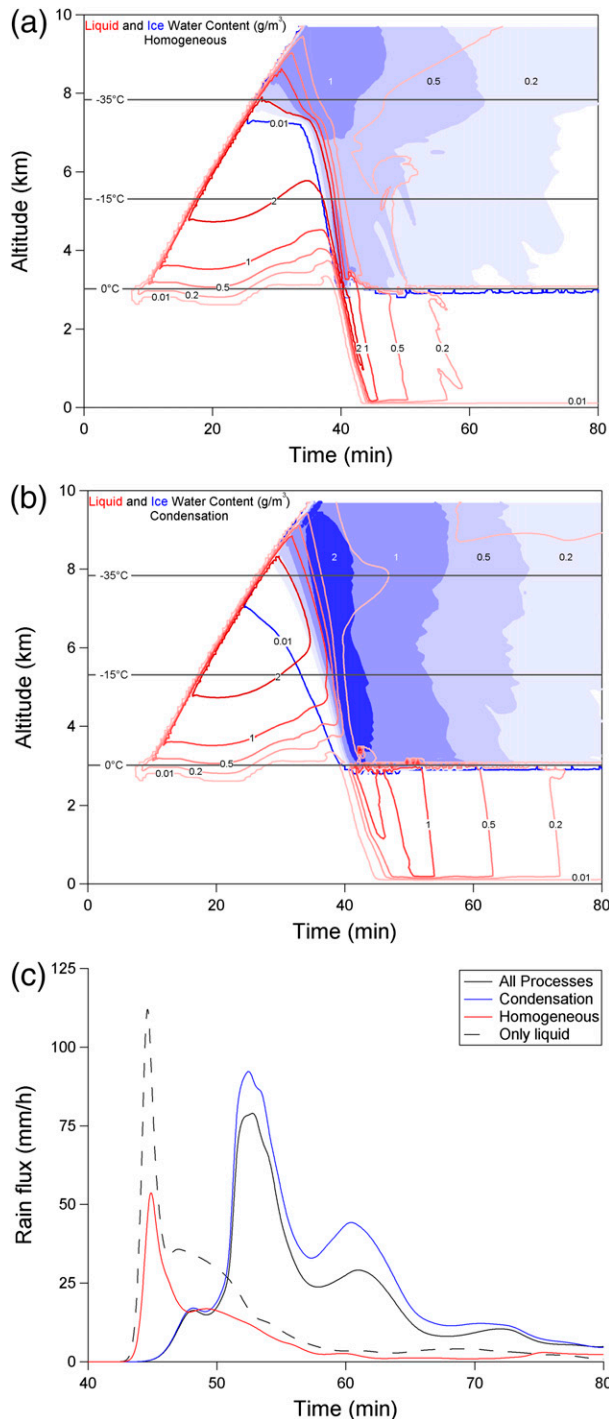


FIG. 4. (a) Liquid water content ( $\text{g m}^{-3}$ ; red) and ice water content ( $\text{g m}^{-3}$ ; blue), simulated with DESCAM as a function of time and height for homogeneous nucleation as the only active ice-forming mechanism (case 6). (b) Liquid water content ( $\text{g m}^{-3}$ ; red) and ice water content ( $\text{g m}^{-3}$ ; blue), simulated with DESCAM as a function of time and height for condensation freezing as the only active ice-forming mechanism (case 7). (c) Time evolution of the rainfall rate ( $\text{mm h}^{-1}$ ) for the reference case (solid black), the all-liquid case (dashed black), the homogeneous nucleation case 6 (red), and the condensation freezing case 7 (blue).

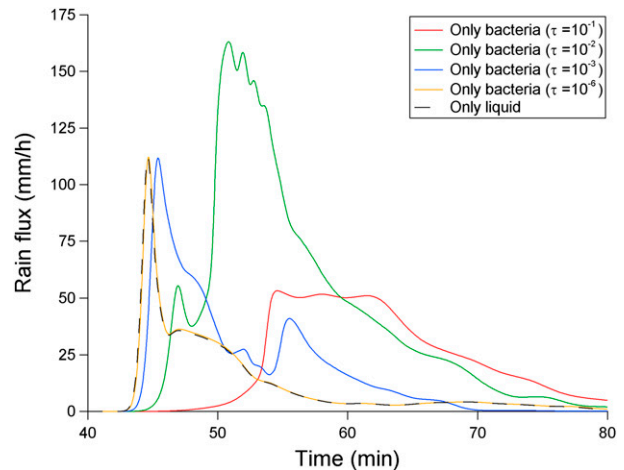


FIG. 5. Time evolution of the rainfall rate ( $\text{mm h}^{-1}$ ) for case 8; the only IN active are *Pseudomonas syringae* 32b-74, which represent a fraction  $\tau$  of the total number of bacteria (aerosol particles of ityp = 2).

drops. The different parameter values will specify how the organization of the water molecules is linked to dissolved or undissolved aerosol particle components, but the resulting rain evolution is somewhat similar (cf. Figs. 3c and 4c).

Compared to these parameterizations, condensation freezing shows a quite contrasting behavior among the ice initiation processes, as it is the only process acting at much warmer temperatures and smaller drop sizes and has, thus, the potential to completely block off the warm rain process. It is associated with important low-level releases of latent heat and, thus, results in the highest precipitation rates. Also, because of the low-level latent heat release and the increased vertical velocity, the condensation freezing parameterization shifted the maximum rainfall intensity to 55 min, as was observed in the reference case (Fig. 4c).

Here, the potential importance of nucleation rates acting on just-formed droplets and IN acting at warmer temperature becomes obvious.

To estimate the potential importance of IN acting at quite warm temperatures, in a final simulation, IN active bacteria were added to the simulation (case 8). Figure 5 displays the resulting rain flux on the ground assuming somewhat unrealistically that the only IN were *Pseudomonas syringae* 32b-74 bacteria that represent a fraction  $\tau$  of the total bacteria present. When only 1% of the bacteria were *Pseudomonas syringae* 32b-74 with the nucleation percentages of Joly et al. (2013) (green curve in Fig. 5), then the total resulting rainfall exceeds even the values from case 7. More or less IN shift the curves of the rain flux significantly. However, a simulation with only *Pseudomonas syringae* 32b-74 as IN is quite

unrealistic. When *Pseudomonas syringae* 32b-74 were added in a simulation where all other IN modes were also forming ice (case 1 + bacteria; not shown), their influence became completely negligible.

## 5. Discussion, conclusions, and outlook

Even though during ice formation in the atmosphere the same thermodynamic principles probably apply to each germ formation and evolution, the associated respective mechanical conditions and sensible and latent heat releases will vary. During the modeling of clouds, the mechanical and heat balance of each individual germ cannot yet be followed individually. Thus, freezing mode parameterizations integrating the exact pathway of interaction between the gaseous, the liquid, and the solid phase during ice formation for finite space and time increments are the only way to treat this process, in particular for the use in bulk microphysical NWP models.

In the current study, different ice-forming parameterizations have been studied in a bin-resolved microphysics model while acting alone and when competing in the simple dynamics of a convective cloud. They influence cloud development and the rain flux on the ground, modifying the integrated values as well as the time evolution. Generally conceived for a particular process, they act on cloud evolution in different ways and, in the studied dynamical framework, have a different overall importance.

For contact freezing to be active, aerosol particles acting as IN have to be present in supercooled conditions together with liquid drops. Because of their size ( $>0.1 \mu\text{m}$ ), IN are generally also CCN and are, thus, easily activated. Consequently, it is not surprising that, in this 1.5D study, contact freezing had a negligible influence. Only a very few ice particles were formed via this mechanism, and the rain on the ground followed very closely through liquid processes alone. Only in a cloud where the cloud base is in subzero regions and supercooled liquid water can exist over extended periods of time outside the cloud could contact freezing potentially increase its importance.

Deposition freezing occurs on unactivated IN in ice-supersaturated regions. Taking into account only deposition freezing as an ice-forming parameterization, the amount of the rain on the ground follows mostly the dynamics of the all-liquid case (Fig. 2c), even though the total number of crystals formed is, in the end, almost as high as for the other cases. In Fig. 6 the cumulative number of formed ice crystals by each nucleation parameterization when acting as the only active mechanism is given. It can be noted that deposition freezing

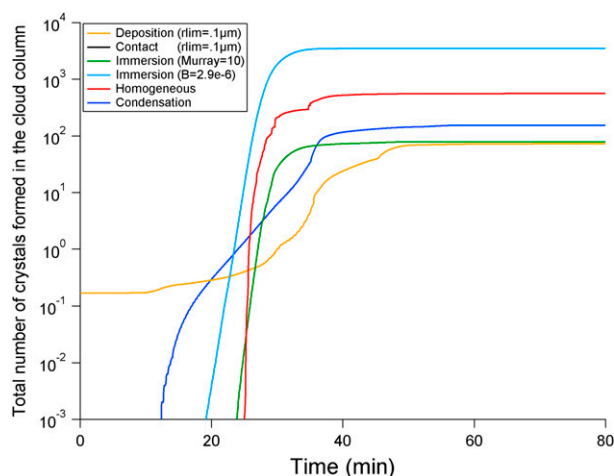


FIG. 6. Cumulative number of nucleated ice crystals for a given mechanism in the total column for the sensitivity cases 3 (deposition), 4 (contact; too low for the drawn scale), 5 (surface and volume immersion), 6 (homogeneous), and 7 (condensation).

(yellow curve) creates ice particles before all other processes do. However, they appear outside the cloud around 8 km and become cloud relevant only when the cloud extends to these altitudes (Fig. 2a). Globally, the number of crystals resulting from deposition freezing during the cloud formation between 10 and 30 min stays below all other mechanisms; it only starts catching up after 40 min because of lateral entrainment processes of fresh IN. However, when combined with other heterogeneous freezing mechanisms, the influence of deposition freezing stays negligible at all times, as can be seen in Figs. 7a and 7b (yellow curve). Here, deposition and contact freezing contribute many fewer crystals than all the other mechanisms. The lower size limit of IN ( $0.1$  or  $0.5 \mu\text{m}$ ) does not affect this result, as the sensitivity tests have demonstrated.

When searching for possible simplifications in models with less complexity, contact and deposition freezing processes can probably be neglected. In more complex models, it needs to be taken into account that IN are large aerosol particles that are generally depleted during cloud formation. Thus, a contribution of deposition or contact freezing inside clouds is highly unlikely.

The overall importance of homogeneous and immersion (surface and volume) freezing is documented in Fig. 6 (when it is the only active ice process) and Figs. 7a and 7b (when it is in competition with other ice-forming processes). To describe homogeneous and volume immersion freezing the parameterization uses, in addition to temperature, the drop volume, and the surface immersion freezing parameterization uses particle surface. Both drop volume and particle surface are parameters that increase with drop age. That these parameters carry

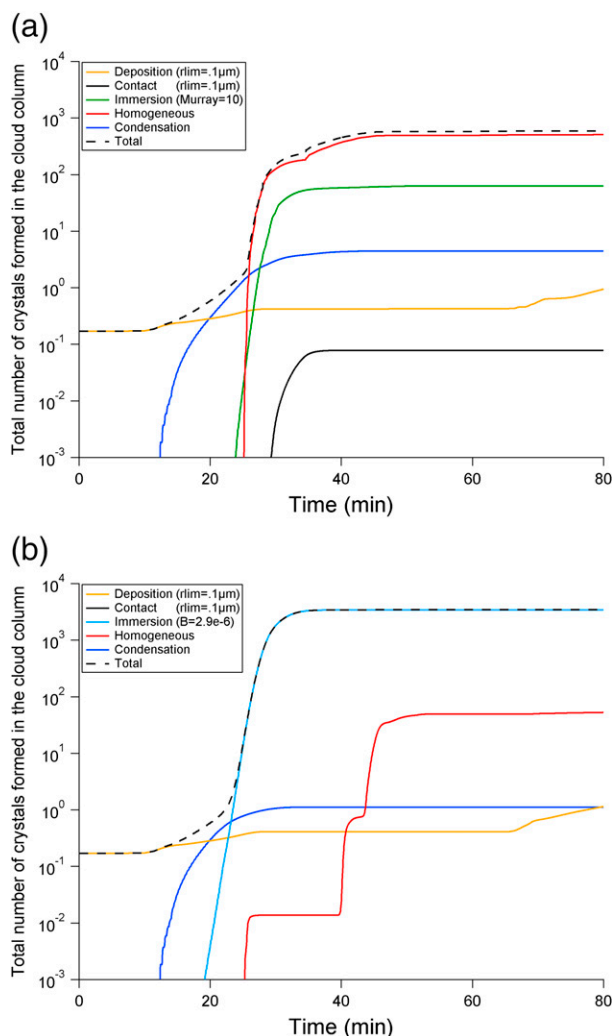


FIG. 7. (a) Cumulative number of nucleated ice crystals in the total column for the different competing processes in case 1 (deposition, surface immersion, homogeneous and condensation freezing, and contact freezing). (b) Cumulative number of nucleated ice crystals in the total column for the different competing processes in case 1 (deposition, volume immersion, homogeneous and condensation freezing; contact freezing is too low for the drawn scale).

the same kind of information was already suggested in the discussion section of Murray et al. (2011). As a function of size, supercooling, and captured impurities, the probability to organize the water molecules in an ice lattice increases. Thus, even though the presence of specific solid IN inside the liquid phase modifies freezing probability, all these freezing parameterizations become important only for altitudes around and above 7 km ( $-30^{\circ}\text{C}$ ) and will, thus, become effective only once the cloud has extended to sufficiently high altitudes and sufficiently large drops have formed (after 20 min). This is confirmed in Fig. 6 by the cumulative number of formed crystals as a function of time when each process

is acting alone. The curves all start rather steep between 20 and 25 min and converge toward a constant value quite rapidly. The light blue curve displaying the volume immersion freezing forms the most ice particles and starts already around 20 min, 5 min prior to homogeneous (red curve) and surface immersion freezing (green curve). At the end of the simulation, homogeneous freezing ice crystal numbers are a factor of 10 lower than the volume freezing rate with the higher  $B$  value and the surface immersion freezing forms overall 100 times fewer crystals. These numbers are caused by the parameters used, since, for example, the immersion volume curve for the lower Bigg values (case 5d, not shown) is quite close to the red curve for homogeneous nucleation (cf. also Figs. 3c and 4c for the impact on surface precipitation). Then the formed ice particles will sedimentate from above into warm microphysics regions and freeze the drops that have formed there through the collision/coalescence process. When the nucleation processes are competing among each other (Figs. 7a,b) the freezing process forming the highest number dominates the overall number of formed crystals. In Fig. 7a homogeneous nucleation dominates, and in Fig. 7b volume immersion freezing dominates (note that immersion volume and immersion surface parameterizations were never used together in a simulation). However, all parameterizations formed ice at cloud top and froze the cloud while falling. Looking for simplifications in models with less complexity, these process parameterizations could probably be lumped together in a unique parameterization, maybe by generalizing an approach similar to the one of Knopf and Alpert (2013).

In comparison with the homogeneous nucleation and immersion freezing, condensation freezing behaves quite differently. It occurs significantly earlier, lower, and at much warmer temperatures. Remember that condensation freezing is limited here to recently formed drops with little overlap with immersion freezing, even though some overlap cannot be excluded. The nucleation of ice starts the riming process (not displayed in the figures), which results in a latent heat release around 6 km, which increases updraft velocities that lengthen cloud and precipitation lifetimes (Figs. 4b,c). Thus, even though the number of crystals formed by condensation freezing is generally smaller than by homogeneous and immersion freezing (cf. Figs. 6, 7), the associated low-level latent heat release invigorates the cloud, extends rainfall duration, and increases its intensity, even in the case of competing ice nucleation processes. This modified dynamics caused by the latent heat release resulted, for example, in the shift of the maximum rainfall intensity to 55 min (Fig. 1c). These results demonstrate that IN that are active at quite warm temperatures and

low altitudes can potentially have quite a large influence on a convective cloud development, in particular as the splintering process, which is also active at these temperatures, could accelerate ice particle production.

Case 8 where all IN were assumed to be *Pseudomonas syringae* 32b-74 with a very high nucleation efficiency showed the potential of warm temperature IN for cloud development. For case 8, none of the above-discussed parameterizations were used. Ice nucleation occurred just as a function of temperature. However, confined to their specific size distribution ( $ityp = 2$ ), their nucleation process corresponds mostly to condensation freezing, which was also confirmed in experiments (Schaupp 2014). Nevertheless, case 8 is highly unrealistic, and the effective role of bacteria as IN has to be studied in competition with all other present IN and an eventual ice multiplication process in a more realistic framework in the future. A very first sensitivity test using a Hallett and Mossop (1974) ice multiplication as described in Leroy et al. (2006) with case 8, however, confirmed the interest of this hypothesis as precipitation increased up to 10% for the  $\tau = 10^{-3}$  case.

Regarding the use of ice initiation mechanisms for larger-scale parameterized models, it becomes obvious that the way the IN mechanism is parameterized is extremely important, as it does not affect the same population of drops. Thus, in addition to IN characteristics and the pure thermodynamic parameters such as temperature, other information on the mechanical and thermal energies involved needs to be recorded to provide a parameterization adapted for cloud process models.

For new simplified nucleation rates to be derived from experiments, our performed sensitivity studies suggest that it seems possible to neglect deposition and contact freezing and to lump homogeneous and immersion freezing together.

Condensation freezing, however, behaves in a distinctively different way than the tested parameterizations for homogeneous, volume, and surface immersion freezing. In the literature for experimental results (e.g., Hoose and Möhler 2012; DeMott et al. 2010) condensation freezing is often grouped with immersion freezing as the necessary time lapse between droplet formation and ice nucleation might seem arbitrary. However, using only immersion freezing rates (cf. case 5) always forms the maximum ice close to cloud top. Only the use of a particular condensation parameterization boosts the formation of ice at midlevel in the cloud (5–6 km), with drastic consequences for cloud and rain dynamics. None of the used immersion freezing parameterizations formed a similar amount of crystals from small drops, even though the rates were applied to all drop sizes. Only the small maximum in the rainfall rate for the high

*B* volume immersion freezing rate (case 5c; Fig. 3c) indicates some nucleation potential for small drops and warm temperatures. The specific use of high-temperature IN, such as bacteria, succeeded in producing similar results to the condensation freezing parameterization. In connection with ice multiplication processes these warm-temperature IN might result in a significant production of low-level ice. Provided that formation of this early ice is admitted to be physical, for the moment, only a specific condensation freezing parameterization, in particular for NWP models, will reproduce this effect.

The consequences for cloud evolution through the different release of latent heat are so important that the two parameterizations should probably be kept separate in cloud models. Parameterization development from experimental studies should, thus, separate the two cloud stages, and an improved parameterization, in particular for the condensation freezing beyond the current dependency on ice supersaturation, is much needed.

Note also that the cumulative IN numbers of Figs. 6 and 7 involved in the different freezing processes do not give the total number of crystals in the ice phase, as the riming process is not displayed here. Riming will convert the formed liquid water into the ice phase through collision with present ice crystals. Riming is a very efficient process that, in most studied cases, rapidly glaciated the entire cloud, even for low IN numbers (e.g., in the case of condensation freezing). The major part of the aerosol particle mass in the ice phase will, thus, enter as a result of drop nucleation (Flossmann and Wobrock 2010) and not because of the IN, which represent much smaller numbers than the CCN (Pruppacher and Klett 1997, chapter 9). In general, it should be kept in mind that IN are a subset of the overall aerosol particle population and will, thus, also be affected by processes such as transport or drop nucleation. To treat them as an always present, separate species will largely overestimate their impact, particularly inside clouds.

The parameterizations of the different ice formation mechanisms that have been used in the model are rather traditional and allow almost no details with respect to the size of the IN and their chemical composition. As mentioned before, the formula of Meyers et al. (1992), which describes condensation freezing, relies only on ice supersaturation. It was arbitrarily assumed here that all particles larger than 0.1 (or 0.5)  $\mu\text{m}$  and smaller than 16  $\mu\text{m}$  have the same probability to serve as IN, where probably the larger IN should be privileged. The same is true for contact freezing, where, in addition, it was assumed that the drop temperature can be described by the air temperature. New measurements of ice

formation on different kinds of particles can be found in the literature; however, to be exploitable for cloud models, they need to be adapted into rates that also parameterize all other eventually occurring subgrid-scale processes. In particular, an improvement of the early condensation freezing rates as a function of nucleus type and size seems important.

Here, the focus was just on an assessment of the overall behavior of each IN mechanism, and we feel relatively confident that the obtained conclusions are independent of the specific parameterizations that were used. However, in order to be completely certain, the robustness of the above recommendations for the role of the different ice nucleation processes needs to be explored further, as well as for different dynamical conditions. Furthermore, the presence of secondary ice multiplication processes will influence cloud evolution, since they seem to occur also at relatively warm temperatures (e.g., Hallett and Mossop 1974). Their influence will be taken into account in future studies.

*Acknowledgments.* The project BIOCLOUDS has been financed by the French INSU/LEFE and the German DFG. One of the authors (AF) acknowledges with gratitude the support provided. The authors want to thank Drs. M. Joly, M. Monier, and C. Schaupp for helpful discussions.

The calculations for this study have been done on computer facilities of the Institut du Développement des ressources en Informatique Scientifique (IDRIS), CNRS at Orsay and the Centre Informatique National de l'Enseignement Supérieur (CINES) at Montpellier under Project 940180. The authors acknowledge with gratitude the hours of computer time and the support provided.

#### REFERENCES

- American Meteorological Society, 2015: "Homogeneous nucleation." Glossary of Meteorology. [Available online at [http://glossary.ametsoc.org/wiki/Homogeneous\\_nucleation](http://glossary.ametsoc.org/wiki/Homogeneous_nucleation).]
- Andraud, M., 2011: Impact of bacteria on cloud life cycle and precipitation. M.S. thesis. Dept. of Atmospheric Physics, University Blaise Pascal, 50 pp.
- Asai, T., and A. Kasahara, 1967: A theoretical study of the compensating downward motions associated with cumulus clouds. *J. Atmos. Sci.*, **24**, 487–496, doi:10.1175/1520-0469(1967)024<0487:ATSOTC>2.0.CO;2.
- Attard, E., H. Yang, A. Delort, P. Amato, U. Pöschl, C. Glaux, T. Koop, and C. Morris, 2012: Effects of atmospheric conditions on ice nucleation activity of *Pseudomonas*. *Atmos. Chem. Phys.*, **12**, 10 667–10 677, doi:10.5194/acp-12-10667-2012.
- Baustian, K. J., D. J. Cziczo, M. E. Wise, K. A. Pratt, G. Kulkarni, A. G. Hallar, and M. A. Tolbert, 2012: Importance of aerosol composition, mixing state, and morphology for heterogeneous ice nucleation: A combined field and laboratory approach. *J. Geophys. Res.*, **117**, D06217, doi:10.1029/2011JD016784.
- Bigg, E. K., 1953: The formation of atmospheric ice crystals by the freezing of droplets. *Quart. J. Roy. Meteor. Soc.*, **79**, 510–519, doi:10.1002/qj.49707934207.
- Burrows, S. M., W. Elbert, M. G. Lawrence, and U. Pöschl, 2009: Bacteria in the global atmosphere—Part 1: Review and synthesis of literature data for different ecosystems. *Atmos. Chem. Phys.*, **9**, 9263–9280, doi:10.5194/acp-9-9263-2009.
- Curry, J. A., and V. I. Khvorostyanov, 2012: Assessment of some parameterizations of heterogeneous ice nucleation in cloud and climate models. *Atmos. Chem. Phys.*, **12**, 1151–1172, doi:10.5194/acp-12-1151-2012.
- Cziczo, D. J., and K. D. Froyd, 2014: Sampling the composition of cirrus ice residuals. *Atmos. Res.*, **142**, 15–31, doi:10.1016/j.atmosres.2013.06.012.
- , and Coauthors, 2013: Clarifying the dominant sources and mechanisms of cirrus cloud formation. *Science*, **340**, 1320–1324, doi:10.1126/science.1234145.
- de Boer, G., T. Hashino, and G. J. Tripoli, 2010: Ice nucleation through immersion freezing in mixed-phase stratoform clouds: Theory and numerical simulations. *Atmos. Res.*, **96**, 315–324, doi:10.1016/j.atmosres.2009.09.012.
- DeMott, P. J., D. C. Rogers, and S. M. Kreidenweiss, 1997: The susceptibility of ice formation in upper tropospheric clouds to insoluble aerosol components. *J. Geophys. Res.*, **102**, 19 575–19 584, doi:10.1029/97JD01138.
- , and Coauthors, 2010: Predicting global atmospheric ice nuclei distributions and their impacts on climate. *Proc. Natl. Acad. Sci. USA*, **107**, 11 217–11 222, doi:10.1073/pnas.0910818107.
- Diehl, K., and S. Wurzler, 2004: Heterogeneous drop freezing in the immersion mode: Model calculations considering soluble and insoluble particles in the drops. *J. Atmos. Sci.*, **61**, 2063–2072, doi:10.1175/1520-0469(2004)061<2063:HDFITI>2.0.CO;2.
- Dye, J. E., and Coauthors, 1986: Early electrification and precipitation development in a small, isolated Montana cumulonimbus. *J. Geophys. Res.*, **91**, 1231–1247, doi:10.1029/JD091iD01p01231.
- Eidhammer, T., and Coauthors, 2010: Ice initiation by aerosol particles: Measured and predicted ice nuclei concentrations versus measured ice crystal concentrations in an orographic wave cloud. *J. Atmos. Sci.*, **67**, 2417–2436, doi:10.1175/2010JAS3266.1.
- Ervens, B., and G. Feingold, 2013: Sensitivities of immersion freezing: Reconciling classical nucleation theory and deterministic expressions. *Geophys. Res. Lett.*, **40**, 3320–3324, doi:10.1002/grl.50580.
- Fletcher, N. H., 1962: *The Physics of Rain Clouds*. Cambridge University Press, 386 pp.
- Flossmann, A. I., 1986: A theoretical investigation of the removal of atmospheric trace constituents by means of a dynamic model. Ph.D. dissertation, Johannes Gutenberg-Universität Mainz, 186 pp.
- , and W. Wobrock, 2010: A review of our understanding of the aerosol–cloud interaction from the perspective of a bin resolved cloud scale modelling. *Atmos. Res.*, **97**, 478–497, doi:10.1016/j.atmosres.2010.05.008.
- Fridlind, A. M., A. S. Ackerman, G. McFarquhar, G. Zhang, M. R. Poellot, P. J. DeMott, A. J. Prenni, and A. J. Heymsfield, 2007: Ice properties of single-layer stratocumulus during the Mixed-Phase Arctic Cloud Experiment: 2. Model results. *J. Geophys. Res.*, **112**, D24202, doi:10.1029/2007JD008646.

- Hallett, J., and S. C. Mossop, 1974: Production of secondary ice particles during the riming process. *Nature*, **249**, 26–28, doi:10.1038/249026a0.
- Hobbs, P. V., 1993: *Aerosol–Cloud–Climate Interactions*. International Geophysics Series, Vol. 54, Academic Press, 233 pp.
- Hoose, C., and O. Möhler, 2012: Heterogeneous ice nucleation on atmospheric aerosols: A review of results from laboratory experiments. *Atmos. Chem. Phys.*, **12**, 9817–9854, doi:10.5194/acp-12-9817-2012.
- , J. E. Kristjánsson, J. P. Chen, and A. Hazra, 2010: A classical-theory-based parameterization of heterogeneous ice nucleation by mineral dust, soot, and biological particles in a global climate model. *J. Atmos. Sci.*, **67**, 2483–2503, doi:10.1175/2010JAS3425.1.
- Jaenicke, R., 1988: Aerosol physics and chemistry. *Landolt-Boernstein: Zahlenwerte und Funktionen aus Naturwissenschaften und Technik*, G. Fischer, Ed., Vol. 4, Springer, 391–457.
- Joly, M., E. Attard, M. Sancelme, L. Deguillaume, C. Guilbaud, C. E. Morris, P. Amato, and A.-M. Delort, 2013: Ice nucleation activity of bacteria isolated from cloud water. *Atmos. Environ.*, **70**, 392–400, doi:10.1016/j.atmosenv.2013.01.027.
- Knopf, D. A., and P. A. Alpert, 2013: A water activity based model of heterogeneous ice nucleation kinetics for freezing of water and aqueous solution droplets. *Faraday Discuss.*, **165**, 513–534, doi:10.1039/c3fd00035d.
- Koop, T., B. Luo, A. Tsias, and T. Peter, 2000: Water activity as the determinant for homogeneous ice nucleation in aqueous solutions. *Nature*, **406**, 611–614, doi:10.1038/35020537.
- Ladino Moreno, L. A., O. Stetzer, and U. Lohmann, 2013: Contact freezing: A review of experimental studies. *Atmos. Chem. Phys.*, **13**, 9745–9769, doi:10.5194/acp-13-9745-2013.
- Leroy, D., M. Monier, W. Wobrock, and A. I. Flossmann, 2006: A numerical study of the effects of the aerosol particle spectrum on the development of the ice phase and precipitation formation. *Atmos. Res.*, **80**, 15–45, doi:10.1016/j.atmosres.2005.06.007.
- Meyers, M. P., P. J. DeMott, and W. R. Cotton, 1992: New primary ice-nucleation parameterizations in an explicit cloud model. *J. Appl. Meteor.*, **31**, 708–721, doi:10.1175/1520-0450(1992)031<0708:NPINPI>2.0.CO;2.
- Monier, M., W. Wobrock, J.-F. Gayet, and A. I. Flossmann, 2006: Development of a detailed microphysics cirrus model tracking aerosol particles histories for interpretation of the recent INCA campaign. *J. Atmos. Sci.*, **63**, 504–525, doi:10.1175/JAS3656.1.
- Morrison, H., M. D. Shupe, J. O. Pinto, and J. A. Curry, 2005: Possible roles of ice nucleation mode and ice nuclei depletion in the extended lifetime of Arctic mixed-phase clouds. *Geophys. Res. Lett.*, **32**, L18801, doi:10.1029/2005GL023614.
- Murray, B. J., S. L. Broadley, T. W. Wilson, J. D. Atkinson, and R. H. Wills, 2011: Heterogeneous freezing of water droplets containing kaolinite particles. *Atmos. Chem. Phys.*, **11**, 4191–4207, doi:10.5194/acp-11-4191-2011.
- , D. O’Sullivan, J. D. Atkinson, and M. E. Webb, 2012: Ice nucleation by particles immersed in supercooled cloud droplets. *Chem. Soc. Rev.*, **41**, 6519–6554, doi:10.1039/c2cs35200a.
- Niemand, M., and Coauthors, 2012: A particle-surface-area-based parameterization of immersion freezing on desert dust particles. *J. Atmos. Sci.*, **69**, 3077–3092, doi:10.1175/JAS-D-11-0249.1.
- Orville, H. D., and F. J. Kopp, 1977: Numerical simulation of the life history of a hailstorm. *J. Atmos. Sci.*, **34**, 1596–1618, doi:10.1175/1520-0469(1977)034<1596:NSOTLH>2.0.CO;2.
- Phillips, V. T. J., and Coauthors, 2009: Potential impacts from biological aerosols on ensembles of continental clouds simulated numerically. *Biogeosciences*, **6**, 987–1014, doi:10.5194/bg-6-987-2009.
- Pruppacher, H. R., and J. D. Klett, 1997: *Microphysics of Clouds and Precipitation*. 2nd ed. Kluwer Academic Publishers, 954 pp.
- Respondek, P. S., A. I. Flossmann, R. R. Alheit, and H. R. Pruppacher, 1995: A theoretical study of the wet removal of atmospheric pollutants: Part V: The uptake, redistribution, and deposition of (NH<sub>4</sub>)<sub>2</sub>SO<sub>4</sub> by a convective cloud containing ice. *J. Atmos. Sci.*, **52**, 2121–2132, doi:10.1175/1520-0469(1995)052<2121:ATSTOW>2.0.CO;2.
- Schaupp, C., 2014: Untersuchungen zur Rolle von Bakterien und Pollen als Wolkenkondensations- und Eiskeime in troposphärischen Wolken. Ph.D. dissertation, Heidelberg University, 169 pp. [Available online at <http://archiv.ub.uni-heidelberg.de/volltextserver/16448/>.]
- Szyrmer, W., and I. Zawadzki, 1997: Biogenic and anthropogenic sources of ice-forming nuclei: A review. *Bull. Amer. Meteor. Soc.*, **78**, 209–228, doi:10.1175/1520-0477(1997)078<0209:BAASOI>2.0.CO;2.
- Tabazadeh, A., S. T. Martin, and J. S. Lin, 2000: The effect of particle size and nitric acid uptake on the homogeneous freezing of aqueous sulfuric acid particles. *Geophys. Res. Lett.*, **27**, 1111–1114, doi:10.1029/1999GL010966.
- Väitilingom, M., E. Attard, N. Gaiani, M. Sancelme, L. Deguillaume, A. I. Flossmann, P. Amato, and A.-M. Delort, 2012: Long-term features of cloud microbiology at the puy de Dôme (France). *Atmos. Environ.*, **56**, 88–100, doi:10.1016/j.atmosenv.2012.03.072.
- Vali, G., 1994: Freezing rate due to heterogeneous nucleation. *J. Atmos. Sci.*, **51**, 1843–1856, doi:10.1175/1520-0469(1994)051<1843:FRDTHN>2.0.CO;2.
- , P. DeMott, O. Möhler, and T. F. Whale, 2014: Interactive comment on “Ice nucleation terminology.” *Atmos. Chem. Phys. Discuss.*, **14**, C9884–C9903. [Available online at <http://atmos-chem-phys-discuss.net/14/C9884/2014/acpd-14-C9884-2014.pdf>.]
- Westbrook, C. D., and A. J. Illingworth, 2013: The formation of ice in a long-lived supercooled layer cloud. *Quart. J. Roy. Meteor. Soc.*, **139**, 2209–2221, doi:10.1002/qj.2096.
- Wright, T. P., and M. D. Petters, 2013: The role of time in heterogeneous freezing nucleation. *J. Geophys. Res. Atmos.*, **118**, 3731–3743, doi:10.1002/jgrd.50365.